# Nonlinearity-induced transition in heat conduction through a topological metamaterial of rotors

T. R. Vishnu and Dibyendu Roy<sup>1</sup>
<sup>1</sup>Raman Research Institute, Bangalore 560080, India

We investigate heat conduction in a one-dimensional chain of rigid rotors. The rotors are constrained to rotate in a plane about fixed pivot points and coupled by springs, such that in equilibrium, the neighboring rotors lie on opposite sides of the chain axis. The linearized limit of this model valid for small angular displacements, was first introduced by Kane and Lubensky (KL) as a topological mechanical insulator hosting zero-energy vibrational edge modes. We show that the linearized KL chain behaves as a thermal insulator at low temperature in both the topological phases with a finite band gap, and the heat current falls exponentially with the chain length. When the gap vanishes at the topological phase transition, the KL chain becomes a good thermal conductor and conducts heat ballistically. The chain of rotors for arbitrary angular displacements hosts nonlinear solitary waves and distinct topological mechanical phases. Our numerical analysis shows normal (diffusive) heat conduction in all topological phases of the nonlinear chain. Nevertheless, a finite thermal conductivity is achieved for different system sizes in different topological phases of this nonlinear chain.

#### I. INTRODUCTION

The concept of topological phases and phase transitions in condensed matter physics originated from the work of Berezinskii, Kosterlitz, and Thouless (BKT) in two spatial dimensional classical XY model or rotor (rotator) model almost fifty years ago [1]. The BKT phase transition has been observed experimentally in thin films of superfluid liquid helium [2], thin disordered superconducting granular films [3, 4], and Josephson junction arrays [5]. The XY or rotor model is invariant under a global continuous rotation of all two-dimensional spins or rotors, a continuous global O(2) symmetry. A decade ago, Kane and Lubensky (KL) [6] introduced another topological model of two-dimensional rotors in one spatial dimension (1D) without the continuous global O(2)symmetry. This linearized model is equivalent to the Su-Schrieffer-Heeger (SSH) model for the electronic excitations of polyacetylene that possesses topologically protected electron states at the free ends or interfaces. The KL model consists of N rigid rotors of mass m and length r, which are constrained to rotate about fixed pivot points on a 1D lattice with spacing a. These rotors are connected by springs with spring constant k so that the alternate rotors in equilibrium make an angle  $\bar{\theta}$  and  $\pi - \bar{\theta}$  with the normal (see Fig. 1). The KL model hosts at least one zero-energy vibrational mode, which can be inferred from the generalized Maxwell's rule.

For small angular displacement of the rotors from their equilibrium position, we can linearize the change in length of the spring between two rotors in terms of angular displacements of these rotors  $(\delta\theta_n, \delta\theta_{n+1})$ . Such a linearized model's vibrational spectrum (phonon modes) under periodic boundary conditions (PBC) consists of acoustic and optical branches. The acoustic branch at a small wavevector is gapped except for specific  $\bar{\theta}$  values. Moreover, the KL model hosts a zero-energy mode for open boundary conditions (OBC), and the mode is ex-

ponentially localized over space at the left or right edge of the rotor chain, depending on  $\bar{\theta}$ . Thus, the linearized model of KL is a topological mechanical insulator since there are no propagating low-energy phonon modes apart from the exponentially localized zero-energy mode below the gap frequency. Using experimental prototypes of the rotor chain, Chen et al. [7], however, demonstrated that when the chain was tilted, a zero (soft) mode initially localized at the edge of the chain propagated under the effect of gravity to the opposite end. Such conduction of zero modes under a mechanical perturbation was argued by going beyond the linearized theory of KL, where the carriers are nonlinear solitary wave excitations. Chen et al. [7] further showed the emergence of different topological solitary waves and phases in the nonlinear model of the chain of rotors. These studies have generated huge research interest, including topological mechanics of gyroscopic metamaterials [8, 9], non-reciprocal topological solitons in active metamaterials [10, 11], and nonlinearity-induced topological phase transitions [12, 13]. The primary purpose of this paper is to investigate the nature of heat conduction in the linear and nonlinear chain of rotors under thermal perturbation from the boundaries.

Heat conduction by phonons in linear and nonlinear low-dimensional lattice models with or without disorder has been extensively explored [14, 15]. It is generally believed that 1D momentum-conserving systems manifest an anomalous heat transport (violating Fourier's law of thermal conduction), where the thermal conductivity diverges as a power-law of system size [16]. A normal (diffusive) heat transport can be attained in momentum nonconserving nonlinear models [17–22]. An exception to the above conjecture is the emergence of diffusive transport in the chain of coupled rotors or 1D classical XY chain with translational and continuous global O(2) invariance [23, 24], which ensures total momentum conservation. Nevertheless, the heat conduction by phonons in topological lattices has not been studied much. We thus

investigated heat conduction in the chain of rotors hosting topological soft modes and connected to two thermal baths at different temperatures at the edges. We analytically derive the heat current in the KL chain, and it falls exponentially with the chain length at low temperature in the topological phases with a finite band gap. This indicates the KL chain acts as a thermal insulator in the topological phases. When the gap vanishes at the topological phase transition, the KL chain becomes a good thermal conductor and conducts heat ballistically. We further numerically explore classical heat conduction in the nonlinear chain of rotors for arbitrary angular displacement. Our analysis shows diffusive heat conduction in the nonlinear chain. However, we find a finite (systemsize independent) thermal conductivity in this nonlinear chain for different chain lengths in different topological phases. Our study reveals a nonlinearity-induced transition from thermal insulator to normal thermal transport in the topological phases of the metamaterial of rotors. The rest of the article is arranged in the following sections and appendices. In Sec. II, we introduce the topological metamaterial of rotors and its topological phases in the linear and nonlinear limit. We discuss heat conduction in the linearized KL chain and nonlinear metamaterial in Sec. III. We briefly summarize our findings and comment on future related studies in Sec. IV. The calculation details of heat conduction in the KL chain is given in App. A.

## II. TOPOLOGICAL METAMATERIAL OF ROTORS

The Hamiltonian of the chain of N rigid rotors for arbitrary angular displacement  $\theta_n$  with the normal (e.g., with the +y axis in Fig. 1) and momentum  $p_n$  at site n can be written as

$$H = \sum_{n=1}^{N} \frac{p_n^2}{2mr^2} + \sum_{n=1}^{N-1} \frac{1}{2}k(l_{n,n+1} - \bar{l})^2,$$
 (1)

where  $\bar{l}$  and  $l_{n,n+1}$  are, respectively, the equilibrium (unstretched) and stretched length of the spring between two neighbouring rotors at n and n+1. We have  $\bar{l} = \sqrt{a^2 + 4r^2\cos^2(\bar{\theta})}$  for all neighbours when the adjacent rotors make the angles  $\theta_n = \bar{\theta}$  and  $\theta_{n+1} = \pi - \bar{\theta}$  for odd n (see Fig. 1). We can further evaluate

$$l_{n,n+1}^2 = a^2 + 2r^2 + 2ar(\sin\theta_{n+1} - \sin\theta_n) -2r^2\cos(\theta_{n+1} - \theta_n).$$
 (2)

Assuming the springs being almost rigid, we can rewrite the potential energy term as

$$\frac{1}{2}k(l_{n,n+1} - \bar{l})^{2} = \frac{1}{2} \frac{k((l_{n,n+1} + \bar{l})(l_{n,n+1} - \bar{l}))^{2}}{(l_{n,n+1} + \bar{l})^{2}} 
\approx \frac{\kappa}{2}(l_{n,n+1}^{2} - \bar{l}^{2})^{2},$$
(3)

where, we approximate  $(l_{n,n+1} + \bar{l})^2 \approx 4\bar{l}^2$  and the renormalized spring constant is  $\kappa = k/4\bar{l}^2$ . Thus, we get the following expression by substituting Eqs. 2 and 3 in Eq. 1:

$$H = \sum_{n=1}^{N} \frac{p_n^2}{2mr^2} + \sum_{n=1}^{N-1} 2\kappa r^4 \left[ \frac{a}{r} (\sin(\theta_{n+1}) - \sin(\theta_n)) - \cos(2\bar{\theta}) - \cos(\theta_{n+1} - \theta_n) \right]^2.$$
(4)

This Hamiltonian was investigated in [7] for explaining

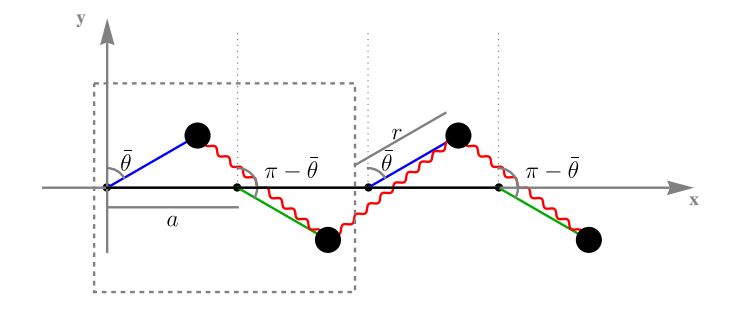


FIG. 1. A cartoon of the topological metamaterial of rotors. The chain is in an equilibrium position, where all rotors have a length r=0.8, and their pivot points are separated by a distance a=1. Out of the four rotors, the rotors at positions x=0,2 (blue) make an angle  $\bar{\theta}=\pi/3$  with the +y axis and the rotors at positions x=1,3 (green) make angle  $\pi-\bar{\theta}=2\pi/3$  with the +y axis. The dotted box represents a unit-cell of the lattice. Since this is a right-leaning configuration, we may able to produce nonlinear solitary waves in this chain by perturbing the right-most rotor (x=3).

the propagation of a soft mode across the chain using a nonlinear conduction mechanism via solitary waves. A linearized version  $(H_{KL})$  of the above Hamiltonian for small angular displacement of the rotors from their equilibrium position was examined by KL [6]. It can be obtained from Eq. 4 by substituting  $\theta_n = \bar{\theta} - \delta\theta_n$ ,  $\theta_{n\pm 1} = \pi - \bar{\theta} - \delta\theta_{n\pm 1}$  and taking the linearized limit  $\cos(\delta\theta_n) \approx 1$  and  $\sin(\delta\theta_n) \approx \delta\theta_n$ .

$$H_{KL} = \sum_{n=1}^{N} \frac{\delta p_n^2}{2mr^2} + \frac{k}{2} \sum_{n=1}^{N-1} (v_1 \delta \theta_n - v_2 \delta \theta_{n+1})^2, \quad (5)$$

$$v_{1,2} = \frac{(2r\sin(\bar{\theta}) \pm a)r\cos(\bar{\theta})}{\sqrt{a^2 + 4r^2\cos^2(\bar{\theta})}},$$
 (6)

where the extension of spring connecting the rotors at site n and n+1 is  $v_1\delta\theta_n - v_2\delta\theta_{n+1}$ . Due to different equilibrium configuration or angle of rotors at even and odd sites of the chain, the chain can be viewed as a lattice with a basis of two sites. Thus, the vibrational spectrum of the chain consists of two branches, namely acoustic and optical branches, which can be obtained by going to Fourier space for PBC. We find the frequencies  $\omega_{\pm}(q_i)$  as

$$\omega_{\mp}^{2}(q_{j}) = \frac{k}{mr^{2}}(v_{1}^{2} + v_{2}^{2} \mp 2v_{1}v_{2}\cos(q_{j}a/2)), \tag{7}$$

where,  $q_j=4\pi j/Na$  for integer  $j\in (-N/4,N/4]$ , with an even numbered of basis. If  $\mathrm{sgn}(v_1)=\mathrm{sgn}(v_2)$  (this means  $2r\sin(\bar{\theta})>a),\ \omega_\mp(q_j)$  are identified as acoustic (-) and optical (+) branches. However, for  $\mathrm{sgn}(v_1)\neq \mathrm{sgn}(v_2)$  (e.g.,  $\bar{\theta}=0,\pi$  correspond to  $v_1=-v_2),\ \omega_+(q_j)$  becomes the acoustic branch. We immediately notice that the acoustic branch is gapped when  $v_1\neq v_2$ , and the gap vanishes when  $|v_1|=|v_2|$  for  $\bar{\theta}=0,\pi$  as  $q_j\to 0$ . The entire phonon spectrum becomes trivially zero at  $\bar{\theta}=\pi/2,3\pi/2$  as  $v_1,v_2$  vanish. For small  $q_j$ , we can express acoustic branch dispersion as  $\omega_+^2(q_j)\approx\omega_0^2+c^2q_j^2$ , where

$$\omega_0^2 = \frac{4kr^2 \sin^2(2\bar{\theta})}{m\bar{l}^2}, \ c^2 = \frac{ka^2(a^2 - 4r^2 \sin^2(\bar{\theta}))\cos^2(\bar{\theta})}{2m\bar{l}^2}.$$
 (8)

For OBC, there is a zero energy mode that is localized at the left or right edge of the KL chain depending on whether the rotors are left-leaning ( $|v_1| < |v_2|$  for  $-\pi < \bar{\theta} < 0$ ) or right-leaning ( $|v_1| > |v_2|$  for  $0 < \bar{\theta} < \pi$ ). The zero mode corresponding to zero potential energy occurs without the stretching or compression of the spring, i.e.,  $\delta l_{n,n+1} = 0$  within the linear approximation. The zero potential energy mode at the left or right edge of the open rotor chain is related to non-zero or zero winding number of the phase of q-space rigidity matrix for PBC when  $\bar{\theta} \neq 0, \pm \pi/2, \pi$ . These topological features of the KL model highlight its similarity with the SSH model.

Nevertheless, there are more intriguing features in the mechanical model in comparison to the electrical model. as Chen et al. [7] points out that the infinitesimal zero potential-energy motion related to the localized topological modes at the edges extends to a finite zero-energy motion that transmits through the bulk of the chain. These finite zero-energy motions represent different solitary waves, which emerge in the presence of nonlinearity. Chen et al. [7] have shown three types of solitary waves [25] in the nonlinear metamaterial, which are moving domain walls between two distinct topological mechanical phases consisting of left- or right-leaning rotors. For  $2(r/a)\sin\bar{\theta} < 1$  in the linkage limit of large spring constant  $(k \gg 1)$ , the passage of a domain wall flips the direction of rotors from  $\theta_n = \bar{\theta}$  to  $\theta_n = -\bar{\theta}$  at odd n. Such a phase of motion in the metamaterial is the flipper phase. In this phase, the entire chain returns to its initial state when the domain wall has moved the chain back and forth twice. For  $2(r/a)\sin\bar{\theta} > 2/\sin\bar{\theta}$ , the rotors rotate counterclockwise by  $\pi$  angle after the passage of a domain wall interpolating between the left- or rightleaning mechanical phases. The emergence of such a domain wall occurs in the spinner phase of the rotor chain. In this case, the rotor chain's initial state is restored after the domain wall has traversed the chain back and forth once. Between these two phases of domain wall motion, there is a special flipper phase, namely a wobbling flipper phase, for  $1 < 2(r/a)\sin\theta < 2/\sin\theta$ , when the rotors go past their equilibrium orientations and oscillate after the passage of a domain wall.

### III. HEAT CONDUCTION

Here, we explore the role of these infinitesimal and finite zero-potential energy motions in heat transport through the chain of rotors. To study heat transport, we connect two Langevin (white noise) heat baths at temperatures  $T_L$  and  $T_R$ , respectively, to the left and right edges of the chain of rotors. It is possible to extract an analytical expression of the heat current in the linearized KL model. We first explore the heat conduction in the linearized model. Later, we numerically explore heat conduction in the nonlinear chain of rotors.

# A. Heat conduction in an open KL chain

An open KL chain for  $\bar{\theta} \neq 0, \pm \pi/2, \pi$  would behave as a thermal insulator at low temperature  $T = (T_L + T_R)/2$  when  $k_B T < \hbar \omega_0$ , since a localized edge mode can not conduct heat. The heat current then falls exponentially with the chain length N. When the gap vanishes for  $\bar{\theta} = 0, \pi$ , the open KL chain will behave as a good conductor and conduct heat ballistically. Thus, the heat current is independent of chain length. We demonstrate these features of heat conduction in an open KL chain by explicitly calculating the exact heat current. For this, we write the quantum Langevin equations of motion for the rotors' angular displacement as follows:

$$mr^{2}\delta\ddot{\theta}_{1} = -kv_{1}^{2}\delta\theta_{1} + kv_{1}v_{2}\delta\theta_{2} - \gamma_{L}\delta\dot{\theta}_{1} + \eta_{L},$$
  

$$mr^{2}\delta\ddot{\theta}_{n} = -k(v_{1}^{2} + v_{2}^{2})\delta\theta_{n} + kv_{1}v_{2}(\delta\theta_{n-1} + \delta\theta_{n+1}),$$
  

$$mr^{2}\delta\ddot{\theta}_{N} = -kv_{2}^{2}\delta\theta_{N} + kv_{1}v_{2}\delta\theta_{N-1} - \gamma_{R}\delta\dot{\theta}_{N} + \eta_{R},(9)$$

where  $n=2,3,\ldots,N-1$ . Here,  $\gamma_{L/R}$  are the coupling strength to the left (L) or right (R) heat baths, and  $\eta_{L/R}$  represent the thermal noise from the left (L) or right (R) baths. We define the heat current from the left heat bath into the KL chain as

$$J_{KL}(t) = -\delta \dot{\theta}_1(t)(-\gamma_L \delta \dot{\theta}_1(t) + \eta_L(t)). \tag{10}$$

We can solve the equations of motion of the rotors in the steady-state by Fourier transforming to frequency to rewrite them in a matrix form as  $Z(\omega)\tilde{\Theta}(\omega) = \tilde{\eta}(\omega)$ , where  $\tilde{\Theta}(\omega) = (\delta\tilde{\theta}_1(\omega), \delta\tilde{\theta}_2(\omega), \cdots, \delta\tilde{\theta}_N(\omega))^T$  and  $\tilde{\eta}(\omega) = (\tilde{\eta}_L(\omega), 0, \cdots, 0, \tilde{\eta}_R(\omega))^T$ . The off-diagonal elements of the tridiagonal matrix  $Z(\omega)$  are  $-kv_1v_2$ , and  $-mr^2\omega^2 + k(v_1^2 + v_2^2)$  are the diagonal elements of  $Z(\omega)$  excluding the first and last elements, which are, respectively,  $-mr^2\omega^2 + kv_1^2 - i\omega\gamma_L$  and  $-mr^2\omega^2 + kv_2^2 - i\omega\gamma_R$ . We define the Fourier transformation as

$$\delta \tilde{\theta}_n(\omega) = \frac{1}{2\pi} \int_{-\infty}^{\infty} dt \delta \theta_n(t) e^{i\omega t}, \tag{11}$$

and similarly for other variables including the noises  $\tilde{\eta}_{L,R}(\omega)$ , which satisfy the following fluctuation-dissipation relations:

$$\langle \tilde{\eta}_b(\omega) \tilde{\eta}_{b'}(\omega') \rangle = \frac{\gamma_b \hbar \omega}{\pi} (1 + f_b) \delta_{b,b'} \delta(\omega + \omega'), \quad (12)$$

where,  $f_b \equiv f(\omega, T_b) = 1/(e^{\hbar\omega/k_BT_b} - 1)$  with b = L, R. Thus, we get the formal solution  $\tilde{\Theta}(\omega) = G(\omega)\tilde{\eta}(\omega)$ , where  $G(\omega) = Z^{-1}(\omega)$  is a retarded Green's function. Using the formal solution, we find the steady-state heat current after taking an average over the noises from the baths as

$$\langle J_{\rm KL} \rangle = \int_{-\infty}^{\infty} d\omega |[G(\omega)]_{1,N}|^2 \gamma_L \gamma_R \frac{\hbar \omega^3}{\pi} (f_L - f_R),$$
 (13)

where  $\langle ... \rangle$  denotes an averaging over the noises. In the linear response regime when  $\Delta T \ll T$  with  $\Delta T = T_L - T_R$ , we can simplify  $\langle J_{\text{KL}} \rangle$  as (assuming  $\gamma_L = \gamma_R = \gamma$ )

$$\langle J_{\rm KL} \rangle = \frac{k_B \Delta T \gamma^2}{\pi} \int_{-\infty}^{\infty} d\omega \left[ |[G(\omega)]_{1,N}|^2 \left( \frac{\hbar \omega^2}{2k_B T} \right)^2 \right] \cos^2 \left( \frac{\hbar \omega}{2k_B T} \right) . \tag{14}$$

An expression of the retarded Green's function to evaluate this integral can be obtained by applying the methods in Refs. [26, 27] for the matrix  $Z(\omega)$  (see App. A 3). We then take a large N limit [28, 29] to find the leading-order T-dependence of  $\langle J_{\rm KL} \rangle$  at low temperatures for the gapped acoustic branch spectrum, e.g.,  $v_1 \neq v_2$  as (see App. A 1)

$$\langle J_{\rm KL} \rangle \sim \frac{e^{-\hbar\omega_0/k_B T}}{\sqrt{T}}, \quad \omega_0 = \sqrt{\frac{k}{mr^2}} (v_1 - v_2). \quad (15)$$

We observe from Eq. 15 that the linearized KL chain behaves as an insulator in the linkage limit of rigid springs  $(k \to \infty)$  at higher temperatures too (even though edge modes are present, they are highly localized). There can be heat conduction in this limit only by going beyond the linear model as explained by Chen et al. [7] for conduction under mechanical perturbation. The linearized KL chain becomes a good conductor even at low temperatures when the acoustic branch becomes gapless, and  $\langle J_{\rm KL} \rangle$  then depends linearly on temperature.

We can also find the N-dependence of  $\langle J_{\rm KL} \rangle$  at low temperatures from Eq. 14 by finding the N-dependence of

 $|[G(\omega)]_{1,N}|^2$  at small frequencies (see App. A 2). We numerically observe that for temperatures below  $\hbar\omega_0$  (i.e.,  $k_BT < \hbar\omega_0$ ),  $\langle J_{\rm KL} \rangle$  is exponentially falling with increasing N for  $v_1 \neq v_2$ . For a relatively large N and a small wavevector q, we can express the Green's function as

$$|G_{1,N}|^2 \approx \frac{m^2 r^4 v_1^2 v_2^2 \sin^2(a\tilde{q})}{((|\tilde{c} + i\tilde{d}(\tilde{q})|) \sin(Na\tilde{q}))^2} \sim e^{\mp 2i(N-1)\tilde{q}},$$
 (16)

where  $2\cos(a\tilde{q}) = -(mr^2\omega^2/kv_1v_2) + (v_1/v_2 + v_2/v_1), \tilde{c} = -(kmr^2v_1v_2 + \gamma^2)(v_1 - v_2)^2, \tilde{d}(q) = (v_1 - v_2)^2\gamma\sqrt{kmr^2(v_1^2 + v_2^2 - 2v_1v_2\cos(a\tilde{q}))}$ . Then, we substitute  $\tilde{q} = \mp i(|v_1 - v_2|)/(a\sqrt{v_1v_2})$  for the zero energy modes of the open KL chain to find  $|G_{1,N}|^2 \sim e^{-2(N-1)|v_1-v_2|/a\sqrt{v_1v_2}}$ . Plugging this form of  $|G_{1,N}|^2$  in Eq. 14, we find  $\langle J_{\rm KL} \rangle$  at low temperatures is decreasing exponentially with N when  $v_1 \neq v_2$ . This further indicates thermal insulating nature of the linear KL chain in the topological phases. We also notice that the quantum current of linear KL model is independent of the system size if  $v_1 = v_2$  (see App. A 2 for details) indicating ballistic transport at low temperatures. In addition, we have numerically verified the system size independence of the quantum current in this gapless regime.

An ordered harmonic chain without spectral gap generally shows ballistic heat conduction (or thermal conductivity linearly diverging with N), which can be argued by the stability of linear Fourier modes and the absence of coupling between conducting modes. No thermal gradient is formed across the system in such a case. We prove rigorously in the App. A 3 that the linear KL chain shows ballistic heat transport at high temperatures  $(k_B T \gg \hbar \omega_0)$  both in the topological phases and the phase transition point. The linear response heat current in Eq. 14 in the high temperature classical limit reads as

$$\langle J_{\rm KL} \rangle^{\rm cl} = \frac{k_B \Delta T \gamma^2}{\pi} \int_{-\infty}^{\infty} d\omega \omega^2 |[G(\omega)]_{1,N}|^2,$$
 (17)

where, we set  $(\hbar\omega/2k_BT)^2 \operatorname{cosech}^2(\hbar\omega/2k_BT) \to 1$ . Applying the expression of the retarded Green's function in App. A 3 at large N limit, we find an analytical expression of  $\langle J_{\rm KL} \rangle^{\rm cl}$  as

$$\langle J_{\rm KL} \rangle^{\rm cl} = \frac{k_B \Delta T k \Gamma^2 \left( 2\gamma^2 \Omega^2 + 2\Gamma^2 \left( 2\gamma^2 - kmr^2 \Omega \right) \left( \sqrt{1 - \frac{4\gamma^4 \Omega^2}{\Gamma^2 (kmr^2 \Omega - 2\gamma^2)^2}} - 1 \right) - 2\gamma^2 \Omega \sqrt{\Omega^2 - 4\Gamma^2} \right)}{4\gamma \Omega \left( \gamma^2 \Omega^2 + \Gamma^2 \left( kmr^2 \Omega - 2\gamma^2 \right) \right)}, \tag{18}$$

where,  $\Omega = v_1^2 + v_2^2$  and  $\Gamma = v_1 v_2$ . The analytical expression matches with the numerical evaluation of the heat current in the KL model at high temperatures.

## B. Heat conduction in the nonlinear metamaterial

For the nonlinear metamaterial, Chen et al. [7] have argued that the flipper and spinner solitary waves can be described by solutions to the  $\phi^4$  and sine-Gordon equations, respectively, which emerge in the continuum limit

of the constraint equation  $\delta l_{n,n+1} = 0$ , when going beyond the linear approximation. Therefore, the nonlinear topological metamaterial is integrable (in the spinner phase), hosting topological solitary waves in the continuum limit. It is imperative to point out that the shape of the solitary waves of the sine-Gordon equation remains invariant under collisions. These special solitary waves are known as solitons. The solitary waves of the  $\phi^4$  equation are not solitons [25]. The integrable models are expected to show ballistic thermal transport due to the presence of nonlinear stable modes (solitons) and complete integrability [22]. Prosen and Campbell [22] showed ballistic heat transport in the spatially discrete version of the sine-Gordon model by Izergin and Korepin, which preserves the integrability of the continuum limit, and it has an on-site potential breaking total momentum conservation. Thus, nonlinear models, even without total momentum conservation, can show non-diffusive heat transport. The existence of an infinite number of independent conserved quantities ensures ballistic transport [30].

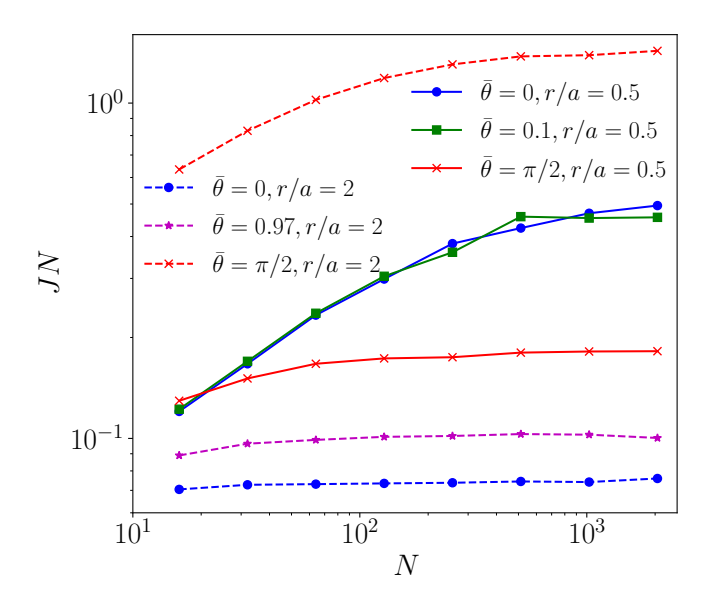


FIG. 2. System-size (N) scaling of JN in a nonlinear metamaterial of rotors for different values of equilibrium angle  $\bar{\theta}$  of the rotors and r/a, where J is steady-state heat current. Other parameters are  $m=k=1, \gamma_L=\gamma_R=0.5, T_L=0.01, T_R=0.5$ . J shows diffusive scaling  $(J\sim N^{-1})$  at longer N for  $\bar{\theta}=0,0.97,\pi/2$  when r/a=2 and  $\bar{\theta}=\pi/2,0.1$  when r/a=0.5. For  $\bar{\theta}=0$  when r/a=0.5, J scales superdiffusively within our finite simulated lengths, and the scaling is  $J\sim N^{-0.85}$ .

The Frenkel–Kontorova model is a nonintegrable (chaotic), discrete version of the sine-Gordon model, and it consists of harmonic nearest-neighbor interactions and a periodic on-site substrate potential, implying the absence of translational invariance or momentum non-conservation. The Frenkel–Kontorova model

and the discrete  $\phi^4$  model show diffusive thermal conduction (or a system-size independent thermal conductivity) [17, 20, 21], which has been used for a general argument for diffusive heat conduction in momentum nonconserving models. The nonlinear metamaterial in Eq. 4 in its discrete form is nonintegrable and chaotic, which is indicated by N-1 positive Lyapunov exponents in different parameter regimes, including the spinner and flipper phases. In fact, positive Lyapunov exponents lead small differences in the initial states to grow exponentially in time, resulting in the development of chaos. Nonintegrable models have shown diffusive and anomalous (superdiffusive) thermal transport depending on the properties of the models and temperature or other parameters [17, 18, 22, 30–40].

We investigate classical heat transport in the nonlinear metamaterial connected to two Langevin heat baths at different temperatures. For this, we numerically evaluate the time-evolution of  $\theta_n(t)$  using the following equations of motion for H in Eq. 4 from some arbitrary initial conditions:

$$mr^2\ddot{\theta}_1 = -\frac{\partial H}{\partial \theta_1} - \gamma_L \dot{\theta}_1 + \eta_L,$$
 (19)

$$mr^2\ddot{\theta}_n = -\frac{\partial H}{\partial \theta_n}, \quad n = 2, 3, \dots, N - 1,$$
 (20)

$$mr^2\ddot{\theta}_N = -\frac{\partial H}{\partial \theta_N} - \gamma_R \dot{\theta}_N + \eta_R,$$
 (21)

where  $\gamma_{L/R}$  are again the coupling strength to the left (L) or right (R) heat baths, and  $\eta_{L/R}$  denote the thermal white noise from the left (L) or right (R) baths, which satisfy the relations in Eq. 12 in the high temperature classical limit. The nonlinear chain reaches a steady state after a transient process over many time steps, which depends on the chain length (e.g.,  $10^7$  steps for  $N \sim 100$ ). We calculate the local heat current at the bond between neighbouring rotors at n, n+1 using the formula

$$J_n(t) = -\dot{\theta}_n \frac{\partial V(\theta_n, \theta_{n+1})}{\partial \theta_n}, \tag{22}$$

where  $V(\theta_n,\theta_{n+1})$  denotes the potential of H in Eq. 4 when rewritten as  $H=\sum_{n=1}^N\frac{p_n^2}{2mr^2}+\sum_{n=1}^{N-1}V(\theta_n,\theta_{n+1}).$  In the steady state of the system, the long-time averaged  $\bar{J}_n$  is independent of n. We take mean of these currents over the full system to find  $J=\sum_{n=1}^{N-1}\bar{J}_n/(N-1).$  The local temperature of  $n^{\rm th}$  rotor can be found from  $T_n=\overline{p_n^2}/(mr^2),$  where the over-line denotes the long-time average.

Since the discrete nonlinear metamaterial is nonintegrable and momentum non-conserving, we expect it to show diffusive thermal transport or  $J \sim N^{-1}$ . We investigate system-size (N)-dependence of the steady-state heat current J in different parameter regimes representing the topological spinner and flipper phase, and the nontopological case of  $\bar{\theta} = 0$ , which corresponds to a gapless acoustic dispersion in the linear KL model. We also consider  $\bar{\theta} = \pi/2$ , where the entire phonon spectrum

of the linear KL model vanishes. Our main findings are shown in Fig. 2, where we plot JN vs. N. It clearly shows JN is a constant for larger N in the spinner phase (e.g.,  $\bar{\theta} = 0.97$  when r/a = 2), indicating diffusive scaling of J as a function of N. This is also the case for  $\bar{\theta} = 0$  when r/a = 2 and  $\bar{\theta} = \pi/2$  when r/a = 0.5. We clearly notice diffusive heat transport in our nonequilibrium simulation, manifested by a constant JN vs. N for larger N values. Further, JN nearly becomes a constant within our simulated lengths for  $\bar{\theta} = \pi/2$  when r/a = 2and in the flipper regime (e.g.,  $\bar{\theta} = 0.1$  when r/a = 0.5). Within our simulated lengths, JN is not a clear constant for  $\bar{\theta} = 0$  when r/a = 0.5. Nevertheless, we expect J to reach diffusive scaling even for these parameters over longer lengths. One exciting feature of JN vs. N plots in Fig. 2 is different length scales, when the diffusive scaling of J emerges in different parameter regimes. We try to understand it by following a small-angle expansion of Haround the equilibrium angle  $\bar{\theta}$ .

We expand H in Eq. 4 in orders of  $\delta\theta_n$  and  $\delta\theta_{n+1}$  using  $\theta_n = \bar{\theta} - \delta\theta_n$ ,  $\theta_{n+1} = \pi - \bar{\theta} - \delta\theta_{n+1}$ . Thus, H simplifies around  $\bar{\theta} = 0$  as

$$H = \sum_{n=1}^{N} \frac{\delta p_n^2}{2mr^2} + \sum_{n=1}^{N-1} 2\kappa r^4 \left[ \frac{a}{r} \left( \delta \theta_n + \delta \theta_{n+1} - \frac{\delta \theta_n^3}{3!} - \frac{\delta \theta_{n+1}^3}{3!} \right) - \frac{(\delta \theta_n - \delta \theta_{n+1})^2}{2} \right]^2.$$
 (23)

We observe significantly different behavior of JN with N in Fig. 2 for r/a=0.5,2 when  $\bar{\theta}=0$ . The coefficients of three terms of potential V in Eq. 23 are significant in determining the thermal transport. These terms are  $(\delta\theta_n+\delta\theta_{n+1})^2, (\delta\theta_n+\delta\theta_{n+1})(\delta\theta_n-\delta\theta_{n+1})^2$  and  $(\delta\theta_n-\delta\theta_{n+1})^4$ . The first term forms the potential of the KL model for  $\bar{\theta}=0$ , leading to a gapless acoustic spectrum and ballistic thermal transport in the KL model. For a small r/a (e.g., r/a=0.5 or a/r=2), the coefficient of the first term is larger than the others. Thus, a longer length-scale is required for the emergence of a constant JN vs. N by relatively weaker nonlinear terms. On the contrary, the coefficient of the second term is larger than the others for r/a=2 or a/r=0.5, which leads to a shorter length-scale for the emergence of a constant JN vs. N by stronger nonlinear terms.

Next, we consider  $\bar{\theta} = \pi/2$ , where we keep only upto the second order terms in the series expansion of trigonometric functions, e.g., sin and cos. Thus, we get

$$H = \sum_{n=1}^{N} \frac{\delta p_n^2}{2mr^2} + \sum_{n=1}^{N-1} 2\kappa r^4 \left[ \frac{a}{r} \left( \frac{\delta \theta_n^2}{2} - \frac{\delta \theta_{n+1}^2}{2} \right) + \frac{(\delta \theta_n - \delta \theta_{n+1})^2}{2} \right]^2.$$
 (24)

It is immediate from Eq. 24 that the first term  $(a/r)(\delta\theta_n^2/2 - \delta\theta_{n+1}^2/2)^2$  in the potential is dominating for smaller r/a, and this term breaks translation symmetry of the model. On the other hand, the translation-

invariant second term in the potential in Eq. 24 dominates for larger r/a. Therefore, the nonlinear metamaterial with  $\bar{\theta}=\pi/2$  is expected to show diffusive behavior within a shorter length for r/a=0.5 compared to r/a=2.

The profile of steady-state local temperature  $T_n$  of the  $n^{\rm th}$  rotor of a nonlinear metamaterial of rotors of length N=1024 is shown in Fig. 3. While we do not find a clear linear  $T_n$  with n in any of these six parameter regimes discussed in Fig. 2, the temperature profile for  $\bar{\theta}=0,0.1$  when r/a=0.5 shows the most deviation from the linear profile, which gives some justification for superdiffusive scaling of J within our finite simulated lengths.

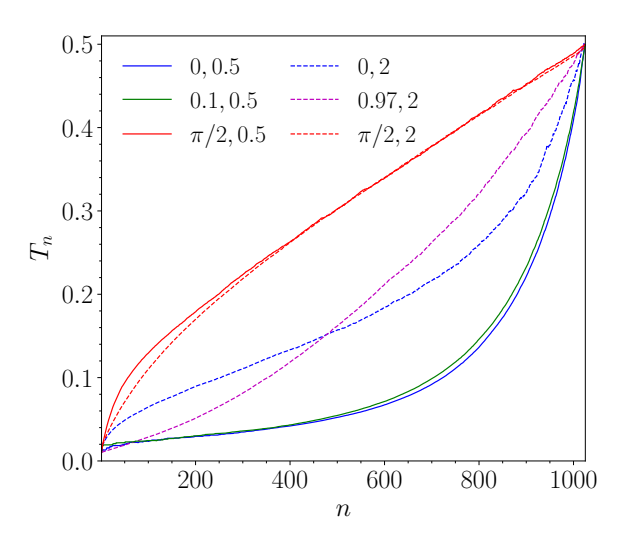


FIG. 3. The profile of steady-state local temperature  $T_n$  of  $n^{\rm th}$  rotor of a nonlinear metamaterial of rotors of length N=1024. The six lines are for different equilibrium angle  $\bar{\theta}$  and r/a as given in the figure. Other parameters are  $m=k=1, \gamma_L=\gamma_R=0.5, T_L=0.01, T_R=0.5$ . The long-time average is taken over  $7\times 10^7$  steps after the transient time of  $7\times 10^7$  steps.

# IV. SUMMARY AND OUTLOOK

In summary, our findings on heat transport in linear and nonlinear metamaterials of rotors are in accordance with the primary features of these metamaterials under mechanical perturbation, namely, a nonlinearity induced transition from insulation to conduction [6, 7]. Chen et al. [7] introduced a classification of topological phases of the nonlinear metamaterials based on the nature of solitary waves. We explicitly calculated the heat current and its scaling with system size in these linear and nonlinear models under thermal perturbation from the boundaries. The heat current in the KL chain decays exponentially with length in the topological phases and is independent of length at the topological phase transition. Thus, the heat current in the linear KL chain can

naturally characterize the topological phases and phase transitions in the KL chain, even though it can not differentiate the two topological phases. On the contrary, the classical thermal transport in nonlinear long chains is not sensitive to the topological phases and phase transitions. We find that the heat current falls linearly with length in different topological phases of Chen et al. [7]. We have not observed any significant difference in the system-size scaling of heat current across these phase boundaries. Even low-temperature classical transport in the nonlinear chain is diffusive, even though it may take a long length scale to achieve such scaling. Therefore, classical thermal transport measurement can not be applied to separate different topological phases of interacting or nonlinear metamaterials. In fact, it is interesting to find out which physical quantity can be used to detect different topological phases of Chen et al. [7]. Studying quantum heat transport in the nonlinear chain is an exciting challenge in this context. The Lyapunov exponents are zero for the KL chain and mostly non-zero in

the nonlinear chain. Analyzing thermal transport in twodimensional systems with anomalous Hall effect behavior or non-reciprocal breathers [10, 11] would also be helpful.

## Appendix A: Heat current in an open KL chain

In this appendix, we derive the temperature and system-size dependence of the quantum heat current of the open KL chain, along with the analytical expression for its high-temperature classical heat current.

# 1. Temperature dependence of quantum heat current

The formal expression of quantum heat current in the linear response regime in Eq. 14 can be expressed in terms of system parameters as (here  $\Omega = v_1^2 + v_2^2$  and  $\Gamma = v_1 v_2$ )

$$\langle J_{\rm KL} \rangle = \frac{\hbar^2 \Delta T}{2\pi k_B T^2} \int_0^{\pi/a} d\tilde{q} \frac{a\gamma k^2 \Gamma^3 \sin^2(a\tilde{q})}{mr^2 (\Gamma(kmr^2\Omega - 2\gamma^2) + 2\Omega\gamma^2 \cos(a\tilde{q}))} \operatorname{cosech}^2\left(\frac{\hbar\omega}{2k_B T}\right). \tag{A1}$$

Here, we re-express  $|G_{1,N}(\omega)|^2$  in terms of the variable  $\tilde{q}$ , which is explained in detail in App. A 3. In the small

 $\tilde{q}$  limit, we have

$$\omega^{2}(\tilde{q}) = \frac{k}{mr^{2}}(v_{1}^{2} + v_{2}^{2} - 2v_{1}v_{2}\cos(a\tilde{q}))$$

$$\approx \frac{k(v_{1} - v_{2})^{2}}{mr^{2}} + \frac{kv_{1}v_{2}a^{2}}{mr^{2}}\tilde{q}^{2} = \omega_{0}^{2} + \lambda\tilde{q}^{2}.(A2)$$

Thus, we re-express Eq. A1 in this limit of small  $\tilde{q}$  as

$$\langle J_{\rm KL} \rangle \approx \frac{2\hbar^2 \Delta T}{\pi k_B T^2} \int_0^{\pi/a} d\tilde{q} \frac{a^3 \gamma k^2 \Gamma^3 \tilde{q}^2 e^{-\hbar \omega_0 / k_B T} e^{-\hbar \lambda \tilde{q}^2 / 2k_B T \omega_0}}{mr^2 (\Gamma(kmr^2 \Omega - 2\gamma^2) + 2\Omega \gamma^2 \cos(a\tilde{q}))}. \tag{A3}$$

Here, we used the approximation  $\operatorname{cosech}^2(\hbar\omega/k_BT) \approx 4e^{\hbar\omega_0/k_BT}e^{-\hbar\lambda\tilde{q}^2/2k_BT\omega_0}$  to get Eq. A3 from Eq. A1. We then substitute

$$x = \frac{\hbar}{k_B T} \sqrt{\frac{k}{mr^2}} \frac{v_1 v_2 a^2 \tilde{q}^2}{(v_1 - v_2)},$$
 (A4)

in Eq. A3 to obtain the leading-order temperature dependence of the quantum heat current, which is given in

Eq. 15, for the gapped case  $v_1 \neq v_2$ .

Similarly, for the gapless case ( $|v_1| = |v_2|$ ), the temperature dependence of  $\langle J_{\rm KL} \rangle$  can be obtained as discussed below. We notice in this case:

$$\omega^2 = \frac{k}{mr^2} (2v_1^2 (1 - \cos(\tilde{q}a))) = \frac{4v_1^2 k}{mr^2} \sin^2\left(\frac{a\tilde{q}}{2}\right). \text{ (A5)}$$
 Thus, a similar analysis like above gives us

$$\langle J_{\rm KL} \rangle = \frac{\hbar^2 \Delta T}{2\pi k_B T^2} \int_0^{\pi/a} d\tilde{q} \frac{a \gamma k^2 \Gamma^2 \sin^2(a\tilde{q})}{2mr^2 (kmr^2 \Gamma - \gamma^2 + 2\gamma^2 \cos(a\tilde{q}))} {\rm cosech}^2 \left( \frac{\hbar \omega}{2k_B T} \right). \tag{A6}$$

By taking the small  $\tilde{q}$  limit, we get

$$\langle J_{\rm KL} \rangle \approx \frac{\hbar^2 \Delta T}{4\pi k_B T^2} \int_0^{\pi/a} d\tilde{q} \frac{a \gamma k^2 \Gamma^2 a^2 \tilde{q}^2}{(k m r^2 \Gamma - \gamma^2 + 2 \gamma^2 - \gamma^2 a^2 \tilde{q}^2)} {\rm cosech}^2 \left( \frac{\hbar \omega}{2 k_B T} \right). \tag{A7}$$

We next substitute  $x = (\hbar \omega)/2k_BT$  in Eq. A7 to find the temperature dependence as  $\langle J_{\rm KL} \rangle \sim T$  when  $v_1 = v_2$ . To obtain this result, we make the assumption  $kmr^2\Gamma - \gamma^2 > 0$ , which is satisfied mostly for small coupling  $\gamma$  compared to the system parameters k, m, r and  $\Gamma$ .

# 2. System-size dependence of quantum heat current

In order to get the N-dependence of  $\langle J_{\rm KL} \rangle$  for  $v_1 \neq v_2$ , we need to find the N-dependence of  $|[G(\omega)]_{1,N}|^2$  at small frequencies. We numerically observe that  $\langle J_{\rm KL} \rangle$  is exponentially falling with N for temperatures below  $\hbar \omega_0$ , i.e.,  $k_B T < \hbar \omega_0$ . To derive this result analytically for the KL chain, we find the following expression for the Green's function when  $\gamma_L = \gamma_R = \gamma$ :

$$|G_{1,N}(\tilde{q})|^2 = \frac{\Gamma^2 m^2 r^4 \sin^2(a\tilde{q})}{\left(\left|(kmr^2 \Gamma^2 - \gamma^2 \Omega) \sin((N-1)a\tilde{q}) + \Gamma(\gamma^2 - kmr^2 \Omega) \sin(Na\tilde{q}) - 2\Gamma \sin(Na\tilde{q})\right)\right.}$$

$$\left. + \Gamma^2 kmr^2 \sin((N+1)a\tilde{q}) + \gamma^2 \Gamma \sin((N-2)a\tilde{q}) + i\gamma mr^2 \sqrt{\frac{k(\Omega - 2\Gamma \cos(a\tilde{q}))}{mr^2}} (\Omega \sin((N+1)a\tilde{q})\right|^2.$$
(A8)

The above in Eq. A8 can be derived following Eqs. A12, A16. For relatively large N (and small  $\tilde{q}$ ), we may simplify Eq. A8 further as

$$|G_{1,N}|^2 \approx \frac{m^2 r^4 \Gamma^2 \sin^2(a\tilde{q})}{\left(\left|(2\Gamma - \Omega)\left(kmr^2\Gamma + \gamma^2 - i\gamma mr^2\sqrt{\frac{k(\Omega - 2\Gamma\cos(a\tilde{q}))}{mr^2}}\right)\right|\sin(Na\tilde{q})\right)^2},\tag{A9}$$

which is  $|G_{1,N}|^2$  in Eq. 16 when  $v_1 \neq v_2$ . We further find that the quantum heat current in the KL chain is independent of N when  $v_1 = v_2$ . We can write the following when  $v_1 = v_2$ :

$$|G_{1,N}(\tilde{q})|^{2} = \frac{m^{2}r^{4}\cos^{2}(a\tilde{q}/2)}{\left(\left|(\gamma^{2} - kmr^{2}\Gamma)\cos((2N - 1)a\tilde{q}/2) - \gamma^{2}\cos((2N - 3)a\tilde{q}/2 + kmr^{2}\Gamma\cos((2N + 1)a\tilde{q}/2)) + i2\sqrt{2}\gamma mr^{2}\sqrt{\frac{k(\Gamma(1 - \cos(a\tilde{q})))}{mr^{2}}}\cos((2N + 1)a\tilde{q}/2))\right|\right)^{2}}.$$
(A10)

For large N, this further simplifies into

$$|G_{1,N}(\tilde{q})|^2 \approx \frac{mr^2 \cos^2(a\tilde{q}/2)}{16\gamma^2 k\Gamma \sin^2(a\tilde{q}/2)\cos(Na\tilde{q})}.$$
 (A11)

For  $|v_1| = |v_2|$ , the acoustic branch is gapless, and the low-energy conducting modes are near  $\tilde{q} \to 0$ , for which  $|G_{1,N}(\tilde{q})|^2$  is almost N-independent. Thus, the quantum heat current in Eq. 14 is system size independent, indicating a ballistic heat transport in the absence of spectral gap at low temperatures.

# 3. Classical heat current

To evaluate  $|G_{1,N}|^2$  in the expression for classical heat current in Eq. 17, we notice that

$$|G_{1,N}|^2 = \frac{1}{\tilde{z}^2 |\det \tilde{Z}|^2}.$$
 (A12)

Here,  $\tilde{z} = kv_1v_2$  and  $\tilde{Z} = Z/\tilde{z}$ , where Z is the tridiagonal matrix define in Sec. III A. Thus, the matrix  $\tilde{Z}$  can be

expressed as

sed as 
$$\frac{z_R}{\tilde{z}} = -\frac{m\omega^2 r^2}{kv_1 v_2} + \frac{v_2}{v_1} - \frac{i\gamma_R \omega}{kv_1 v_2} = \frac{z}{\tilde{z}} - \epsilon_R,$$

$$\frac{z}{\tilde{z}} = -\frac{m\omega^2 r^2}{kv_1 v_2} + \frac{v_1}{v_2} + \frac{v_2}{v_1},$$

$$\frac{z}{\tilde{z}} = -\frac{m\omega^2 r^2}{kv_1 v_2} + \frac{v_1}{v_2} + \frac{v_2}{v_1},$$

$$\frac{z}{\tilde{z}} = -\frac{m\omega^2 r^2}{kv_1 v_2} + \frac{v_1}{v_2} + \frac{v_2}{v_1},$$

$$(A14)$$

$$\vdots \qquad \cdots \qquad \cdots \qquad \cdots \qquad \vdots$$

$$\vdots \qquad \cdots \qquad \cdots \qquad \cdots \qquad \vdots$$

$$\vdots \qquad \cdots \qquad \cdots \qquad \cdots \qquad \vdots$$

$$\vdots \qquad \cdots \qquad \cdots \qquad \cdots \qquad \vdots$$

$$\vdots \qquad \cdots \qquad \cdots \qquad \cdots \qquad \vdots$$

$$\vdots \qquad \cdots \qquad \cdots \qquad \cdots \qquad \vdots$$

$$\vdots \qquad \cdots \qquad \cdots \qquad \cdots \qquad \cdots \qquad \vdots$$

$$\vdots \qquad \cdots \qquad \cdots \qquad \cdots \qquad \cdots \qquad \vdots$$

$$\vdots \qquad \cdots \qquad \cdots \qquad \cdots \qquad \cdots \qquad \vdots$$

$$\vdots \qquad \cdots \qquad \cdots \qquad \cdots \qquad \cdots \qquad \vdots$$

$$\vdots \qquad \cdots \qquad \cdots \qquad \cdots \qquad \cdots \qquad \vdots$$

$$\vdots \qquad \cdots \qquad \cdots \qquad \cdots \qquad \cdots \qquad \vdots$$

$$\vdots \qquad \cdots \qquad \cdots \qquad \cdots \qquad \cdots \qquad \vdots$$

$$\vdots \qquad \cdots \qquad \cdots \qquad \cdots \qquad \cdots \qquad \vdots$$

$$\vdots \qquad \cdots \qquad \cdots \qquad \cdots \qquad \cdots \qquad \vdots$$

$$\vdots \qquad \cdots \qquad \cdots \qquad \cdots \qquad \cdots \qquad \vdots$$

$$\vdots \qquad \cdots \qquad \cdots \qquad \cdots \qquad \cdots \qquad \vdots$$

$$\vdots \qquad \cdots \qquad \cdots \qquad \cdots \qquad \cdots \qquad \vdots$$

$$\vdots \qquad \cdots \qquad \cdots \qquad \cdots \qquad \cdots \qquad \vdots$$

$$\vdots \qquad \cdots \qquad \cdots \qquad \cdots \qquad \cdots \qquad \vdots$$

$$\vdots \qquad \cdots \qquad \cdots \qquad \cdots \qquad \cdots \qquad \vdots$$

$$\vdots \qquad \cdots \qquad \cdots \qquad \cdots \qquad \cdots \qquad \vdots$$

$$\vdots \qquad \cdots \qquad \cdots \qquad \cdots \qquad \cdots \qquad \vdots$$

$$\vdots \qquad \cdots \qquad \cdots \qquad \cdots \qquad \cdots \qquad \vdots$$

$$\vdots \qquad \cdots \qquad \cdots \qquad \cdots \qquad \cdots \qquad \vdots$$

$$\vdots \qquad \cdots \qquad \cdots \qquad \cdots \qquad \cdots \qquad \vdots$$

$$\vdots \qquad \cdots \qquad \cdots \qquad \cdots \qquad \cdots \qquad \cdots \qquad \vdots$$

$$\vdots \qquad \cdots \qquad \cdots \qquad \cdots \qquad \cdots \qquad \cdots \qquad \vdots$$

$$\vdots \qquad \cdots \qquad \cdots \qquad \cdots \qquad \cdots \qquad \cdots \qquad \cdots \qquad \vdots$$

$$\vdots \qquad \cdots \qquad \cdots$$

$$\vdots \qquad \cdots \qquad \cdots$$

Here, the matrix elements have the following form

$$\frac{z_L}{\tilde{z}} = -\frac{m\omega^2 r^2}{kv_1 v_2} + \frac{v_1}{v_2} - \frac{i\gamma_L \omega}{kv_1 v_2} = \frac{z}{\tilde{z}} - \epsilon_L, \qquad \text{with } \epsilon_L = (v_2/v_1) + (i\gamma_L \omega/kv_1 v_2) \text{ and } \epsilon_R = (v_1/v_2) + (i\gamma_R \omega/kv_1 v_2).$$

In order to find det  $\tilde{Z}$ , we use the substitution  $(z/\tilde{z}) = 2\cos(a\tilde{q})$ . If we allow  $\tilde{q} = 2\pi n/Na$ , with  $n = 1, \dots, N$ , then we notice that

$$\omega^2(\tilde{q}) = \frac{k}{mr^2} (v_1^2 + v_2^2 - 2v_1 v_2 \cos(a\tilde{q})), \tag{A15}$$

gives all frequencies in the acoustic and optical branches given in Eq. 7. Note that each branches consist of N/2 frequencies. The small  $\tilde{q}$  behaviour of Eq. A15 is the same as that of the acoustic branch in Eq. 7 with the same band gap, when  $v_1 \neq v_2$ . With this substitution, the determinant can be expressed as

$$\det[\tilde{Z}_N] = \Delta_N = \frac{A(\tilde{q})\sin(Na\tilde{q}) + B(\tilde{q})\cos(Na\tilde{q})}{\sin(a\tilde{q})}.$$
(A16)

Here,

$$A(\tilde{q}) = -(\epsilon_L + \epsilon_R) + (1 + \epsilon_L \epsilon_R) \cos(a\tilde{q}) \quad \text{and} \quad B(\tilde{q}) = (1 - \epsilon_L \epsilon_R) \sin(a\tilde{q}). \tag{A17}$$

For  $\gamma_L = \gamma_R = \gamma$ , we find

$$A(\tilde{q}) = \frac{-k(v_1^2 + v_2^2)}{kv_1v_2} + \left(2 - \frac{\gamma^2\omega^2}{(kv_1v_2)^2}\right)\cos(a\tilde{q}) + i\left(\frac{k\gamma\omega(v_1^2 + v_2^2)\cos(a\tilde{q})}{(kv_1v_2)^2} - \frac{2\gamma\omega}{kv_1v_2}\right),\tag{A18}$$

and

$$B(\tilde{q}) = \left(\frac{\gamma^2 \omega^2}{(k v_1 v_2)^2}\right) \sin(a\tilde{q}) + i \left(\frac{k \gamma \omega (v_1^2 + v_2^2) \sin(a\tilde{q})}{(k v_1 v_2)^2}\right). \tag{A19}$$

Thus, the square of the determinant can be expressed as

$$|\Delta_N|^2 = \frac{(|A|^2 + |B|^2)(1 + r_1 \sin(2Na\tilde{q} + \phi))}{2\sin^2(a\tilde{q})},$$
(A20)

with  $r_1 \cos \phi = (AB^* + A^*B)/(|A|^2 + |B|^2)$  and  $r_1 \sin \phi = (|B|^2 - |A|^2)/(|A|^2 + |B|^2)$ . Now using Eq. A15, we get the classical heat current in the KL chain:

$$\langle J_{\rm KL} \rangle^{\rm cl} = \frac{k_B \Delta T}{\pi} \left( \frac{k}{mr^2} \right)^{3/2} \frac{4\gamma^2}{k^2 v_1 v_2} \int_0^{\pi/a} d\tilde{q} \frac{a \sin^3(a\tilde{q}) \sqrt{v_1^2 + v_2^2 - 2v_1 v_2 \cos(a\tilde{q})}}{(|A|^2 + |B|^2)(1 + r_1 \sin(2Na\tilde{q} + \phi))}. \tag{A21}$$

In the large N limit, using the identity

$$\lim_{N \to \infty} \int_0^{\pi} d\tilde{q} \frac{g_1(\tilde{q})}{1 + g_2(\tilde{q})\sin(N\tilde{q})} = \int_0^{\pi} d\tilde{q} \frac{g_1(\tilde{q})}{(1 - g_2(\tilde{q})^2)^{1/2}},\tag{A22}$$

along with the identifications  $g_2(\tilde{q}) = r_1$ , and

$$g_1(\tilde{q}) = \frac{a\sin^3(a\tilde{q})\sqrt{v_1^2 + v_2^2 - 2v_1v_2\cos(a\tilde{q})}}{(|A|^2 + |B|^2)},$$
(A23)

and noticing that

$$(1 - g_2(\tilde{q})^2)^{1/2} = \frac{2(|a_1b_2 - a_2b_1|)}{|A|^2 + |B|^2},\tag{A24}$$

we get the classical heat current

$$\langle J_{\rm KL} \rangle^{\rm cl} = \frac{k_B \Delta T}{\pi} \left( \frac{k}{mr^2} \right)^{3/2} \frac{2\gamma^2}{k^2 v_1 v_2} \int_0^{\pi/a} d\tilde{q} \frac{a \sin^3(a\tilde{q}) \sqrt{v_1^2 + v_2^2 - 2v_1 v_2 \cos(a\tilde{q})}}{(|a_1 b_2 - a_2 b_1|)}. \tag{A25}$$

Here,  $A = a_1 + ia_2$  and  $B = b_1 + ib_2$ . Thus, we have

$$|a_1b_2 - a_2b_1| = \frac{\gamma \left(\frac{k}{mr^2}(v_1^2 + v_2^2 - 2v_1v_2\cos(a\tilde{q}))\right)^{3/2} \left(v_1v_2(kmr^2(v_1^2 + v_2^2) - 2\gamma^2) + 2(v_1^2 + v_2^2)\gamma^2\cos(a\tilde{q})\right)\sin(a\tilde{q})}{k^3v_1^4v_2^4}.$$
 (A26)

Applying this in the above expression, we get the classical heat current in terms of the system parameters as

$$\langle J_{\rm KL} \rangle^{\rm cl} = \frac{k_B \Delta T}{\pi} \int_0^{\pi/a} \frac{d\tilde{q} \, 2a \sin^2(a\tilde{q}) \gamma k \Gamma^3}{(\Omega - 2\Gamma \cos(a\tilde{q}))(\Gamma(kmr^2\Omega - 2\gamma^2) + 2\Omega\gamma^2 \cos(a\tilde{q}))}. \tag{A27}$$

Here,  $\Omega = v_1^2 + v_2^2$  and  $\Gamma = v_1 v_2$ . By a change of variable  $x = \cos(a\tilde{q})$ , we re-express the heat current as

$$\langle J_{\rm KL} \rangle^{\rm cl} = \frac{k_B \Delta T}{\pi} \int_{-1}^{1} \frac{2\gamma k \Gamma^3 \sqrt{1 - x^2} \, dx}{(\Omega - 2\Gamma x)(\Gamma(kmr^2\Omega - 2\gamma^2) + 2\Omega\gamma^2 x)}.$$
 (A28)

We thus get the analytical form of the classical heat current in Eq. 18, when  $2\Omega\gamma^2 < \Gamma(kmr^2\Omega - 2\gamma^2)$ . In the special case of  $\bar{\theta} = 0$  (i.e.,  $v_1 = v_2$  implying  $\Omega = 2\Gamma$ ), this formula can be further simplified to

$$\langle J_{\rm KL} \rangle^{\rm cl} = \frac{k_B \Delta T \Gamma k \left( 4\gamma^2 + 2 \left( \gamma^2 - \Gamma k m r^2 \right) \left( \sqrt{1 - \frac{4\gamma^4}{(\gamma^2 - \Gamma k m r^2)^2}} - 1 \right) \right)}{8 \left( \gamma^3 + \gamma \Gamma k m r^2 \right)}. \tag{A29}$$

- [1] D. Thouless, *Topological Quantum Numbers in Nonrelativistic Physics* (World Scientific, 1998).
- [2] D. J. Bishop and J. D. Reppy, Study of the superfluid transition in two-dimensional <sup>4</sup>He films, Phys. Rev. Lett. 40, 1727 (1978).
- [3] A. F. Hebard and A. T. Fiory, Evidence for the Kosterlitz-Thouless transition in thin superconducting aluminum films, Phys. Rev. Lett. 44, 291 (1980).
- [4] K. Epstein, A. M. Goldman, and A. M. Kadin, Vortexantivortex pair dissociation in two-dimensional superconductors, Phys. Rev. Lett. 47, 534 (1981).
- [5] D. J. Resnick, J. C. Garland, J. T. Boyd, S. Shoe-maker, and R. S. Newrock, Kosterlitz-Thouless transition in proximity-coupled superconducting arrays, Phys. Rev. Lett. 47, 1542 (1981).
- [6] C. L. Kane and T. C. Lubensky, Topological boundary modes in isostatic lattices, Nat. Phys. 10, 39–45 (2013).
- [7] B. G. Chen, N. Upadhyaya, and V. Vitelli, Nonlinear conduction via solitons in a topological mechanical insulator, Proc. Natl. Acad. Sci. U.S.A. 111, 13004–13009 (2014).
- [8] L. M. Nash, D. Kleckner, A. Read, V. Vitelli, A. M. Turner, and W. T. M. Irvine, Topological mechanics of gyroscopic metamaterials, Proc. Natl. Acad. Sci. U.S.A.

**112**, 14495 (2015).

- [9] P. Wang, L. Lu, and K. Bertoldi, Topological phononic crystals with one-way elastic edge waves, Phys. Rev. Lett. 115, 104302 (2015).
- [10] J. Veenstra, O. Gamayun, X. Guo, A. Sarvi, C. V. Meinersen, and C. Coulais, Non-reciprocal topological solitons in active metamaterials, Nature 627, 528 (2024).
- [11] J. Veenstra, O. Gamayun, M. Brandenbourger, F. van Gorp, H. Terwisscha-Dekker, J.-S. Caux, and C. Coulais, Nonreciprocal breathing solitons, Phys. Rev. X 15, 031045 (2025).
- [12] K. Sone, M. Ezawa, Y. Ashida, N. Yoshioka, and T. Sagawa, Nonlinearity-induced topological phase transition characterized by the nonlinear Chern number, Nat. Phys. 20, 1164 (2024).
- [13] K. Sone, M. Ezawa, Z. Gong, T. Sawada, N. Yoshioka, and T. Sagawa, Transition from the topological to the chaotic in the nonlinear Su–Schrieffer–Heeger model, Nat. Commun. 16, 422 (2025).
- [14] S. Lepri, R. Livi, and A. Politi, Thermal conduction in classical low-dimensional lattices, Phys. Rep. 377, 1 (2003).
- [15] A. Dhar, Heat transport in low-dimensional systems,

- Adv. Phys. 57, 457–537 (2008).
- [16] O. Narayan and S. Ramaswamy, Anomalous heat conduction in one-dimensional momentum-conserving systems, Phys. Rev. Lett. 89, 200601 (2002).
- [17] B. Hu, B. Li, and H. Zhao, Heat conduction in onedimensional chains, Phys. Rev. E 57, 2992 (1998).
- [18] T. Hatano, Heat conduction in the diatomic Toda lattice revisited, Phys. Rev. E 59, R1 (1999).
- [19] G. P. Tsironis, A. R. Bishop, A. V. Savin, and A. V. Zolotaryuk, Dependence of thermal conductivity on discrete breathers in lattices, Phys. Rev. E 60, 6610 (1999).
- [20] B. Hu, B. Li, and H. Zhao, Heat conduction in onedimensional nonintegrable systems, Phys. Rev. E 61, 3828 (2000).
- [21] K. Aoki and D. Kusnezov, Bulk properties of anharmonic chains in strong thermal gradients: non-equilibrium  $\phi^4$  theory, Physics Letters A **265**, 250 (2000).
- [22] T. Prosen and D. K. Campbell, Normal and anomalous heat transport in one-dimensional classical lattices, Chaos 15, 015117 (2005).
- [23] C. Giardinà, R. Livi, A. Politi, and M. Vassalli, Finite thermal conductivity in 1d lattices, Phys. Rev. Lett. 84, 2144 (2000).
- [24] O. V. Gendelman and A. V. Savin, Normal heat conductivity of the one-dimensional lattice with periodic potential of nearest-neighbor interaction, Phys. Rev. Lett. 84, 2381 (2000).
- [25] P. M. Chaikin and T. C. Lubensky, *Principles of Condensed Matter Physics* (Cambridge University Press, 1995).
- [26] A. Dhar and D. Roy, Heat transport in harmonic lattices, J. Stat. Phys. 125, 801 (2006).
- [27] G. Y. Hu and R. F. O'Connell, Analytical inversion of symmetric tridiagonal matrices, J. Phys. A: Math. Gen. 29, 1511 (1996).
- [28] D. Roy and A. Dhar, Heat transport in ordered harmonic

- lattices, J. Stat. Phys. 131, 535 (2008).
- [29] T. R. Vishnu and D. Roy, Heat transport through an open coupled scalar field theory hosting stability-toinstability transition, J. Stat. Phys. 191, 123 (2024).
- [30] H. van Beijeren, Exact results for anomalous transport in one-dimensional hamiltonian systems, Phys. Rev. Lett. 108, 180601 (2012).
- [31] G. Casati, J. Ford, F. Vivaldi, and W. M. Visscher, Onedimensional classical many-body system having a normal thermal conductivity, Phys. Rev. Lett. 52, 1861 (1984).
- [32] T. Prosen and M. Robnik, Energy transport and detailed verification of Fourier heat law in a chain of colliding harmonic oscillators, J. Phys. A 25, 3449 (1992).
- [33] S. Lepri, R. Livi, and A. Politi, Heat conduction in chains of nonlinear oscillators, Phys. Rev. Lett. 78, 1896 (1997).
- [34] S. Lepri, R. Livi, and A. Politi, On the anomalous thermal conductivity of one-dimensional lattices, EPL 43, 271 (1998).
- [35] S. Lepri, R. Livi, and A. Politi, Energy transport in anharmonic lattices close to and far from equilibrium, Physica D 119, 140 (1998).
- [36] A. Dhar, Heat conduction in a one-dimensional gas of elastically colliding particles of unequal masses, Phys. Rev. Lett. 86, 3554 (2001).
- [37] A. V. Savin, G. P. Tsironis, and A. V. Zolotaryuk, Heat conduction in one-dimensional systems with hard-point interparticle interactions, Phys. Rev. Lett. 88, 154301 (2002).
- [38] P. Grassberger, W. Nadler, and L. Yang, Heat conduction and entropy production in a one-dimensional hard-particle gas, Phys. Rev. Lett. 89, 180601 (2002).
- [39] G. Casati and T. Prosen, Anomalous heat conduction in a one-dimensional ideal gas, Phys. Rev. E 67, 015203 (2003).
- [40] D. Roy, Crossover from Fermi-Pasta-Ulam to normal diffusive behavior in heat conduction through open anharmonic lattices, Phys. Rev. E 86, 041102 (2012).